Demonstration of Quantum Channel Monitoring via Quantum Wrappers

Mehmet Berkay On,[1] Sandeep Kumar Singh,[1] Gamze Gul,[2] Gregory S. Kanter,[2] Roberto Proietti,[3] Prem Kumar,[2] and S. J. Ben Yoo[1,*]

[1]*Department of Electrical and Computer Engineering, University of California, Davis, CA, 95616, USA*
[2]*Department of Electrical and Computer Engineering, Northwestern University, Evanston, IL, 60208, USA*
[3]*Dipartimento di Elettronica e Telecomunicazioni, Politecnico di Torino, Torino, 10129, Italy*

[*]*sbyoo@ucdavis.edu*

Abstract: We experimentally demonstrate quantum channel monitoring by wavelength-time multiplexing of classical wrapper bits with quantum payloads. Bit-error-rate measurements of 5 Gb/s classical bits infer the coincidence-to-accidental ratio of the quantum channel up to 13.3 dB. © 2023 The Author(s)

1. Introduction

Recent progress in quantum technologies promises to revolutionize classical computing and information-processing techniques. While quantum computers would be able to solve problems that are exponentially difficult for classical computers [1], quantum key distribution (QKD) offers to achieve unconditional security [2]. As a result, *quantum internet* emerges, which interconnects quantum network clients [3]. A fiber-optic infrastructure is a potential candidate to support the development of quantum networks because of its low-loss transmission of photons, passive wavelength routing, abundant bandwidth, and readily available massive deployment [4, 5]. Quantum bits (qubits) and entangled photons are the basic unit of quantum information, the analogue of classical bits. However, qubits are fragile, unlike classical bits. This nature of qubits challenges future quantum networks to manage network monitoring, switching, routing, etc., without destroying qubits. Thus, we proposed the Quantum Wrapper Networking (QWN) [6]. The fundamental concept of QWN is inspired by optical label switching [7]. It is designed for transparent and interoperable transportation of QW datagrams consisting of quantum payloads, classical header, and optionally tail bits. QW headers include source-destination ID, qubit duration, quantum application type, entanglement type, etc. QW headers are read either at the edge node or at the routers. QW routers switch and regenerate QW headers to transmit quantum payload end-to-end without measuring or disturbing qubits. Fig.1 shows a point-to-point link, where QW headers and payloads are both time and wavelength multiplexed. Quantum transmitter (TX) generates broadband polarization entangled photon pairs. Single photon receivers (RX) on the both side of the link perform qubit measurements. Although QWN does not require trusted nodes, quantum repeaters, and qubit processing at the router, QW Header transcievers (TRX) and single photon TRX should be accurately synchronized.

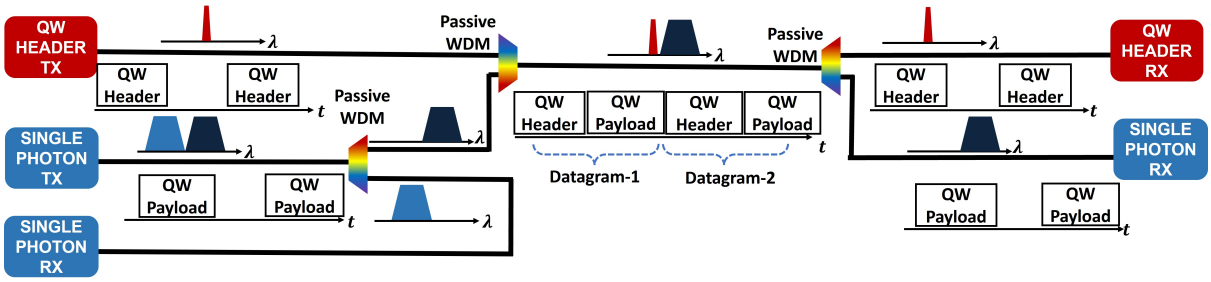

Fig. 1. A schematic of the point-to-point WDM QW datagram transmission

Our previous work investigated wavelength-division multiplexed (WDM) continuous wrapper bits coexisting with the continuously transmitted qubits [8]. In this work, we implement quantum wrapper (QW) datagrams consisting of burst-mode classical header bits and quantum payloads. We measure coincidence counts and calculate the coincidence-to-accidental ratio (CAR) as a quality metric for the quantum channel. The CAR quantifies the signal-to-noise ratio (SNR) of the coincidence counts of orthogonal polarization basis. We observe that with burst-mode headers, the CAR significantly improves to 12.6 dB (Fig.3. e)), compared to 3.7 dB with continuous QW

headers (Fig.3. c)). Additionally, we demonstrate that the wrapper bit-error-rate (BER) is correlated with qubits' CAR. Therefore we can infer quantum channel quality via the QW datagram's header BER without altering the quantum payloads.

2. Experimental Setup & Results

We implement QW datagrams experimentally by the setup in Fig. 2 a). For the header bits, we use a small-form-factor pluggable TX operating at the wavelength of 1561.42 nm, 5 Gbps data rate, and $2^{10}-1$ pseudo-random bit sequence. An external lithium niobate Mach-Zehnder modulator (MZM) gates the continuous classical data stream to realize burst-mode headers. The extinction ratio of the MZM is ∼12 dB. A field-programmable gate array (FPGA) board generates multiple synchronous electrical signals to drive the MZM, gate the error analyzer (EA) and the time-to-digital converter (TDC) circuit. Fig.2 b) shows the optical output from the built burst TX on the scope. Fig.2 c) and Fig.2 d) shows the gating signals for the EA, the single-photon detectors (SPD), and the TDC. A 1.23 ms QW datagram period consists of 1.13 ms quantum payload, and 102.4 μs QW header. An electrical polarization controller (EPC) scrambles the polarization of the burst TX. An optical tunable filter (OTF) suppresses the ASE spectrum from the TX, and a variable optical attenuator (VOA) controls the launch power of the classical TX into the coexistence channel.

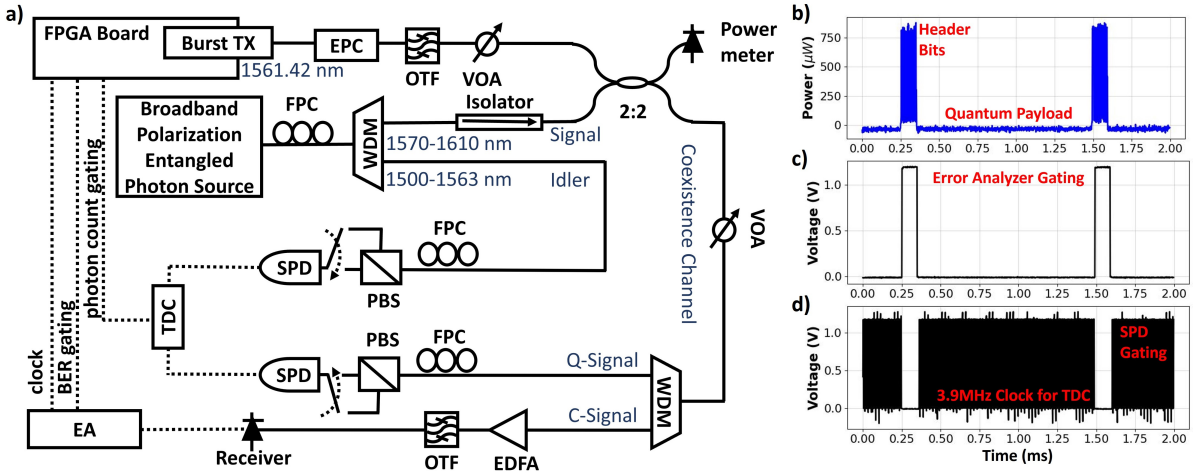

Fig. 2. a) Schematic of the experimental setup. b) Optical output of the burst TX. c) Electrical signal from FPGA board to gate EA. d) Electrical signal from FPGA to gate SPD and clock TDC.

We use a broadband polarization-entangled photon source (EPS-1000 from OZ Optics) based on a periodically-poled silica fiber. The EPS is continuously pumped at 782.86 nm and generates entangled pairs centered around 1565.72 nm. A thin film coating based 3-port WDM multiplexer separates entangled photon pairs, *signal* at L-band and *idler* at C-band. Header bits are coupled with the quantum signal by a 2-by-2 power coupler. Another VOA emulates different possible values of the coexistence channel attenuation. Another WDM device demultiplexes classical and quantum signals. The demultiplexed classical signal is preamplified and detected by an optical receiver. LYNXEA-NIR InGaAs avalanche photodiodes (from AureaTechnology) as SPDs with a built-in TDC measure the coincidence counts. Although the EPS continuously generates qubits, we gate the TDC only during the quantum payload period to emulate the packetized quantum payload. Fiber-based polarization controllers (FPC) are aligned to the horizontal (H) and vertical (V) polarization axis of the polarization beam splitters (PBS).

We record four measurements (HH, HV, VH, and VV) for both continuous and burst-mode header bits at TX launch power -21 dBm. Header BER is <1E-12 at this power level. The CAR is computed by the formula $CAR = (CC_{(HV,VH)}/CC_{(HH,VV)})$ as a quality of quantum channel metric [9]. Fig.3. c) and e) show coincidence counts in 100 seconds for continuous and burst modes, respectively. Due to the -50 dB crosstalk of the demultiplexing WDM device, CAR of the qubits degrades significantly, 3.7 dB for continuous headers. With time-division multiplexing, the burst-mode operation can achieve 12.6 dB. We recorded 16.1 dB CAR without any classical signal power, Fig.3. b). Therefore, a higher extinction ratio MZM could further improve the CAR with the burst-mode operation. TX launch power is decreased to -28 dBm, where burst-mode BER is 1.2E-10 to observe the relation between QW header BER and QW payload CAR. Fig.3 a) shows BER and CAR w.r.t. coexistence channel attenuation. The attenuation in the channel degrades the QW headers SNR and causes higher BER. Similarly, CAR as *Quantum SNR* decreases with increasing channel attenuation. Therefore, in this case, QW header BER can infer

quantum channel quality without directly measuring qubits. Lastly, we place a 5 km SMF-28 fiber in the coexistence channel and measure the coincidence counts in burst mode, Fig.3. f). Coincidence count distribution in time shifts ∼24.4 μs, and its variance increases due to SMF's group velocity dispersion. The fiber transmission impairments require further investigation in future works.

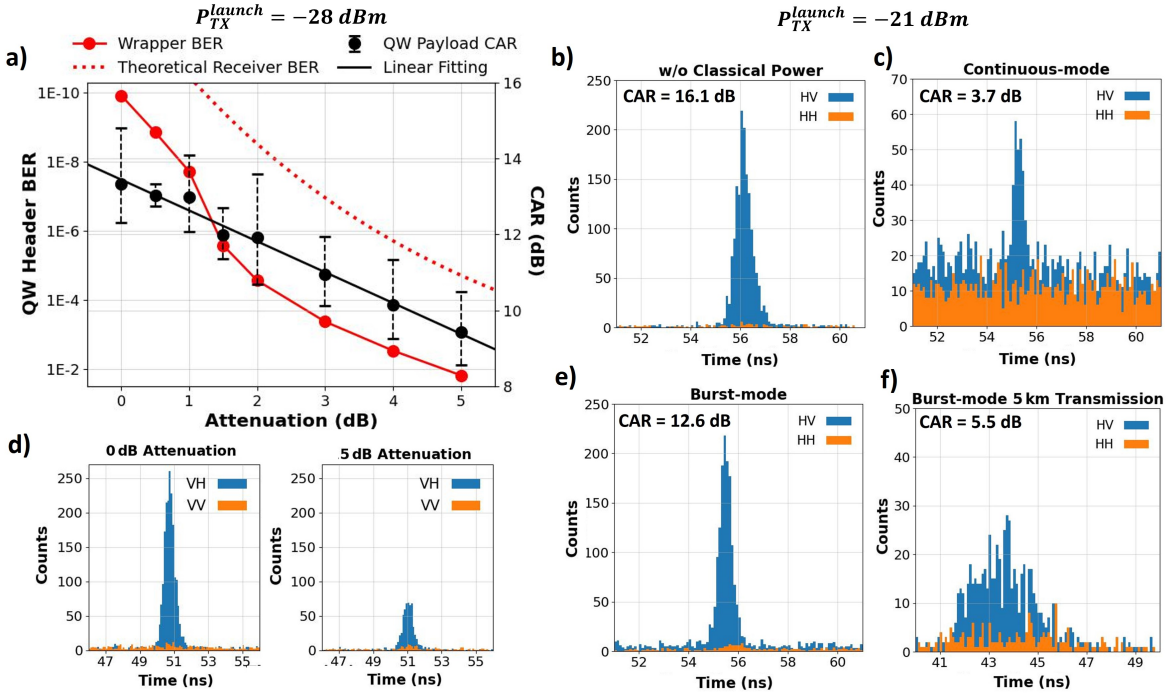

Fig. 3. a) Header BER and qubit CAR vs. channel attenuation at -28 dBm TX launch power. b) Coincidence counts w/o classical power at -21 dBm TX launch power. c) Coincidence counts with WDM continous headers at -21 dBm TX launch power. d) Coincidence counts for 0 dB and 5 dB channel attenuation at -28 dBm TX launch power. e) Coincidence counts with WDM burst-mode headers at -21 dBm TX launch power. f) Coincidence counts for WDM burst-mode headers with 5 km SMF-28 transmission at -21 dBm TX launch power.

3. Conclusion

We demonstrate packetized transmission of the QW datagrams in a point-to-point link. Furthermore, we conclude that QW header BER can give insight into quantum channel quality without measuring qubits. In future works, we plan to use the QW headers to monitor qubit entanglement fidelity and switch the quantum payloads when a specific QW header is detected.

4. References

1. F. Arute *et al.*, "Quantum supremacy using a programmable superconducting processor," Nat. 2019 574:7779 **574**, 505–510 (2019).
2. V. Scarani *et al.*, "The security of practical quantum key distribution," Rev. Mod. Phys. **81**, 1301–1350 (2009).
3. S. Wehner, D. Elkouss, and R. Hanson, "Quantum internet: A vision for the road ahead," Science **362** (2018).
4. S. Lloyd *et al.*, "Infrastructure for the quantum Internet," Comput. Commun. Rev. **34**, 9–20 (2004).
5. J. Chung *et al.*, "Illinois express quantum network (ieqnet): Metropolitan-scale experimental quantum networking over deployed optical fiber," (2021).
6. S. J. Ben Yoo and P. Kumar, "Quantum Wrapper Networking," 2021 IEEE Photonics Conf. IPC 2021 - Proc. (2021).
7. S. J. Yoo, "Optical packet and burst switching technologies for the future photonic internet," J. Light. Technol. **24**, 4468–4492 (2006).
8. S. Singh, M. On, R. Proietti, G. Kanter, P. Kumar, and S. Yoo, "Experimental demonstration of correlation between copropagating quantum and classical bits for quantum wrapper networking," ECOC (2022).
9. C. Liang, K. F. Lee, M. Medic, P. Kumar, R. H. Hadfield, and S. W. Nam, "Characterization of fiber-generated entangled photon pairs with superconducting single-photon detectors," Opt. Express **15**, 1322–1327 (2007).

This work is supported by the U.S. DOE, Office of ASCR program under Award Number DE-SC-0022336.